Cooperative Autonomy of Multiple Solar-Powered Thermaling Gliders ⋆

Nahum Camacho, ∗
Vladimir N. Dobrokhodov, Kevin D. Jones, ∗∗

∗ *Graduate student at the Department of Mechanical and Aerospace
Engineering, Naval Postgraduate School, Monterey, CA 93943 USA
(e-mail: ncamacho@nps.edu)*
∗∗ *Research Associate Professors at the Department of Mechanical and
Aerospace Engineering, Naval Postgraduate School, Monterey, CA
93943 USA (e-mail: vndobrok, kdjones@nps.edu)*

Abstract: This paper presents a review of the multidisciplinary approach to the design of a fleet of cooperative gliders capable of extended endurance operation. The flock of autonomous gliders is able to harvest energy from the environment, both through photo-voltaic energy generation and through exploitation of natural convective lift in the surrounding air, and act cooperatively to meet mission requirements and to share knowledge of the local environment. The paper begins with a brief overview of the total-energy approach required for such a feat, along with a short description of key system components and the principal technologies. This is followed by details of the evolution of a previously-developed architecture that supported autonomous thermaling, to an architecture that considers the total-energy budget in all flight segments, and utilizes the cooperative flight to maximize the cumulative energy capture while simultaneously meeting mission objectives.

Keywords: cooperative control; solar energy; convective air energy; autonomous soaring; UAV.

1. INTRODUCTION

One of the most critical limiting factors impacting effective collaborative autonomy today is the lack of range and endurance that are typical in most of the existing autonomous aircraft; see a comprehensive review in Committee on Autonomous Vehicles in Support of Naval Operations [2005]. Despite almost two decades of significant advances in low-power and high-performance microelectronics development including CPUs, sensors, actuators, and communication circuits Tong [1995], Singh and Shukla [2010], the only task addressed was to lower the power consumption and to reduce the pace of energy expenditures. In turn, the progress in energy renewable technologies has also been advancing fast, especially in the flight-relevant areas of solar photovoltaics (Hamakawa [2004]) and electro-chemical battery technologies, see Tarascon and Armand [2001]. Yet, the balance of energy use and the regenerated energy income has not been met. Since the loss of energy is unavoidable due to the limited efficiency of energy conversion, storage, and transmission, the traditional mission duration will always be limited. However, coupling these existing advances with convective air (thermal) soaring capabilities and novel approaches in the cooperative mission planning and execution can not only further reduce the rate of loss of onboard energy, but can also result in energy increase during the autonomous

mission; this capability is not readily available today in any of the available technologies, see Siciliano and Khatib [2008], Martinez et al. [2008], and Nonami et al. [2013].

Considering the state of the art in aerial robotics (algorithmic support, instrumentation, size weight and power constraints), it is our belief that the best approach to enable long duration flight would combine the collaborative mission management with the energy harvesting and onboard storage. Collaboration is the first key capability that spans across every element of the mission as it enables effective search for available energy sources. Most of the available energy sources can be detected by autonomous vehicles equipped with appropriate sensors. Thus, multiple agents would have much better chances of finding ”free energy“ when cooperating and sharing their findings. Second, the operational utility of multiple agents equipped with complementary sensors is superior to the capability of an individual agent. Finally, robustness of the collaborative mission execution is significantly higher because partial loss of a subset of the vehicles does not lead to the loss of entire flock capability. Energy harvesting and storage is the second complementary enabler of long endurance flight that allows for the accumulation of energy. The feasible methods of energy extraction in aerial application include the solar PV and airflow soaring; the soaring can be based on the convective air (thermaling) or wind shear energy extraction. While the PV boost can be achieved only during the daylight, the extraction of power of surrounded moving air can be utilized even during the

nighttime. The combination of harvesting and storage is the ultimate solution for the "eternal" flight.

Therefore, it is envisioned that enhancing mission performance can be achieved by implementing the energy harvesting-storage and collaboration capabilities onboard of multiple autonomous solar-powered and thermal-soaring gliders. Thus, the triplet of (*i*) mission management, (*ii*) energy harvesting-storage and (*iii*) collaboration builds the fundamental architecture of future energy enhanced autonomy. The remainder of the paper briefly outlines the core ideas implemented to date in autonomous thermaling. Therefore, the section 2 describes the "individual gliders" algorithms. The following section 3 outlines the development of the collaborative autonomy algorithms. Section 4 provides details of the developed high-fidelity simulation environment used to verify the algorithms.

2. ALGORITHMS OF INDIVIDUAL GLIDERS

This section discusses key components necessary for a successful glider flight. The algorithms run online and enable *identification of the flight dynamics* of the glider which are in turn used to *detect the thermal updrafts*. When flying in the updraft, the *guidance algorithm* is engaged to enable the maximum energy harvesting efficiency of the updraft's free energy, and on the other hand *estimates the updraft geometry and motion*, that are used to georeference the updraft and share its utility properties (strength) across the network of collaborative gliders. While in autonomous soaring mode, the *electrical management* system that consists of solar PV panels, batteries and the maximum peak power energy tracking (MPPT) unit, supports the avionics and recharges the batteries keeping them evenly balanced.

2.1 Electric Energy Management Subsystem

The project considers two sources of energy input into the system: photovoltaic (PV) and atmospheric convection, and typically two methods of energy storage; potential energy stored chemically in batteries and potential energy stored via altitude. This section describes the electrical half of that system; electricity harvesting through PV conversion and energy storage in rechargeable batteries.

While the electrical system architecture is conceptually well-understood, the variation of physical and mechanical properties of PV panels and batteries presents the most significant uncertainty, and thus poses the challenge for the overall system design. Not only basic physical properties of all components vary significantly, but also the same properties depend on the mode of operation (e.g. discharge rate) and environmental parameters(e.g. temperature). Thus, before the electrical system is integrated onboard it is necessary to characterize mathematically the solar-powered energy generation, storage, and the energy expenditure system, so that the particular uncertain parameters could be identified on the ground and during the flight of a particular glider platform. The need for online identification arises as the properties of the system are expected to change over time.

As an example, the following data represent the results of the discharge experiment performed with 2 different types of batteries at different discharge rates; the experiment

Table 1. Measured battery performance

Type	C-rate	Energy (Wh)	Energy Density (Wh/kg)
LiPo	0.209	115.5	177.7
LiPo	2.502	105.8	162.8
LiIon	0.171	107.9	167.3

utilized the Lithium polymer (LiPo) and the Lithium-Ion (LiIon) packs. Figure.1 illustrates how voltage drops over the discharge cycle, a feature that is convenient for estimating remaining energy in the battery pack.
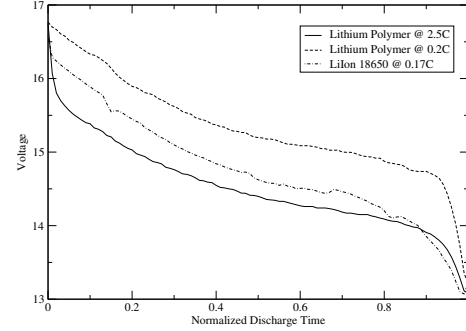

Fig. 1. Pack voltage as a function of normalized discharge time for 2 different chemistries of the battery packs at different discharge rates.

Figure.2 illustrates how much energy can be extracted from the same sample batteries at different discharge rates. During the experiment, the discharge cycles were halted when the pack voltage reached 3.2 V/cell or 12.8 V for the pack. The measured useful pack energy and energy-density are shown in Table 1. While the sensitivity to drain rate
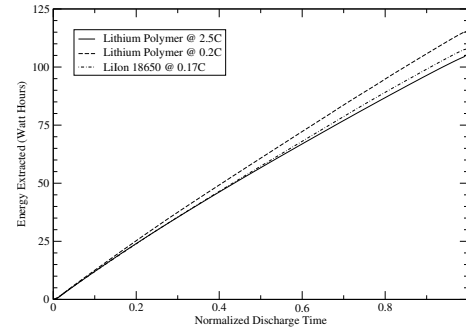

Fig. 2. Energy output as a function of normalized discharge time for different discharge rates; at 1C rate the discharge current discharges the battery in 1 hour.

is clear, it is also clear that advertised energy and energy-density might not be achievable in a practical application. While the LiIon cells would appear to be far superior based on manufacturers' specifications, experiments suggest that LiPo batteries are superior for onboard integration.

A number of other uncertainties and design considerations still need to be identified and formalized. Among them are the structural integrity of the wings and the PV cells under the flex load in flight, dissipation of heat induced by the dark surface of solar panels and its effect of the structural integrity, performance of the MPPT unit under the variable exposure of the PV cells to the sun, stability of the battery chemistry under variable temperature, losses in the mechanical gear system and the propulsion motors

at different load, to name a few. Moreover, it is needless to say that PV-enhanced system may gain energy, however it won't help if the aircraft loses that same energy through increased viscous drag or loss of lift. Therefore the cells need to be built into the wing surface such that they are conformal with only subtle fine-texture differences.

Addressing this challenge, the projects built a generalized prototype of the onboard system that consists of the semi-rigid research-grade mono-crystalline Silicon cells with an advertised efficiency of 22.5%, MPPT unit, rechargeable batteries with balancing circuitry, and the load represented by the well-defined power load of avionics and the uncertain load of the propulsion system. An example of the laboratory prototype used for multi-day data acquisition and system identification experiment is presented in Figure. 3.
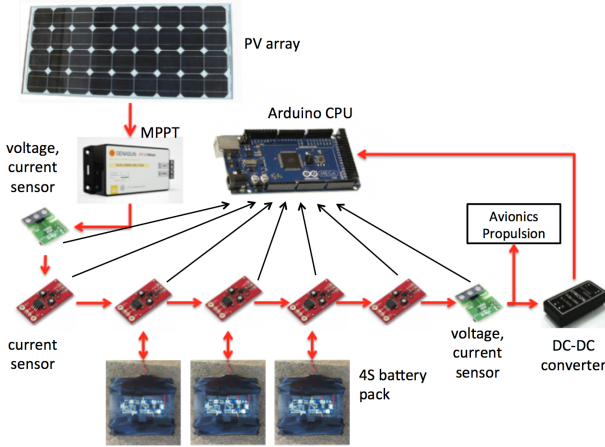

Fig. 3. Laboratory prototype of the solar-driven electrical management system; the setup is instrumented with a set of voltage and current sensors at key points to allow for the system identification.

An example of multi-day experiment focusing on acquiring data for precise characterization of the system is presented next in Figure.4. The data represents the time history of electrical energy input from the PV array, the dynamics of the batteries charge and discharge under the constant load, and the estimated losses of energy due to the wiring, data acquisition sensors and adverse uncertainties. Close inspection of the data suggests that the state dynamics of batteries (both charge and discharge) can be accurately described by the first order differential equations, while the solar input is closely represented by the gain that is directly proportional to the angle of incidence toward the sun. Although not representing all the envisioned flight conditions, the result still allows to recognize the key functions that can be used to formally describe the states of the key system components and the total electrical energy balance. When the result is further enhanced with the feedback from the flight dynamics and the operational environment, it can be used to precisely characterize the range and endurance of a particular glider platform. The system identification phase of this work is under way.

2.2 Glider Identification and Updraft Detection

There is a number of prior efforts devoted to the thermal soaring flight. First demonstrated by human pilots in 1900s (see Simons and Schweizer [1998]) the idea of soaring in
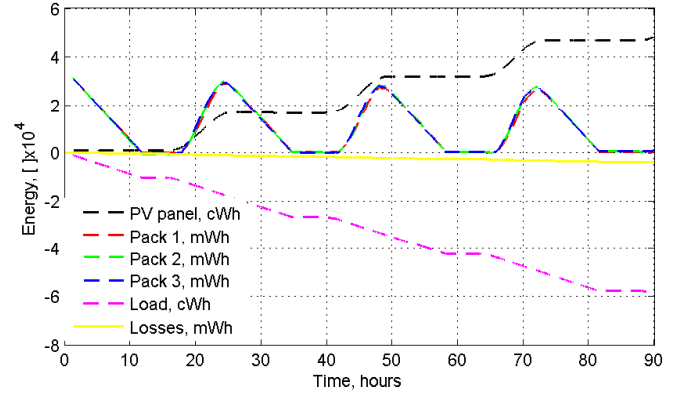

Fig. 4. Results of the multi-day experiment with the prototype installed in a fixed location.

convective air became feasible for onboard autonomous implementation only in the 1990s, see Wharington [1998]. While enabling the desired functionality by primarily mimicking the birds flight and indeed achieving significant extended flight capabilities (see Edwards [2008], Allen [2006] and Allen and Lin [2007]), most of the algorithms used heuristics in the identification of the updraft strength, its potential utility in energy gain, and the decision of when and how to enter the updraft. The reason for employing heuristic approaches is obvious, since both the strength of the updraft and its efficiency are both subject to significant uncertainties and are hard to formalize. Next, when a glider moves through unsteady air the estimation of the updraft strength and geometry, which are critical utility parameters of the updraft, significantly lacks of spatial content in noisy onboard measurements. Thus, it takes significant time before the updraft utility is identified and the guidance algorithm is engaged.

The algorithm of detecting a thermal is based on two complementary approaches. The first approach utilizes the inherent sink rate polar, and the second one is based on the total energy of the system. However, conceptually they are similar as they compare the natural metrics of the system with the same metrics actually measured in flight.

Characterization of the sink polar - the function of vertical sink rate versus the true airspeed (TAS) of an aircraft - of a particular glider can be practically achieved in extensive experimentation. However, flight-experimentation in real-world environment can hardly provide ideally controlled conditions. In the developed approach, the estimates of the sink-polar were first made by post-processing a collection of experimental flight results obtained in low-wind, low-lift conditions, see Andersson et al. [2012b]. Sink polars are roughly quadratic in nature, and a least-squares approach yields suitable coefficients based on the historical data. Further in flight, a recursive linear least square (see Astrom and Wittenmark [1975]) estimator is used in real-time to account for specific variation in the platform and atmospheric conditions at that moment. An example of accuracy of this approach is presented below in Figure.5 for a full-scale ASW-27 glider; the result was obtained using the Condor simulator (Condor [2013]) and "true" data of Boermans and Van Garrel [1994], see more details in sec.4. The detection of a thermal based on the sink polar is based

on comparison of the currently measured sink rate with the sink rate predicted by the polar for a given TAS measurements; if the measured sink rate is smaller then predicted then there is a thermal. The analytical representation of
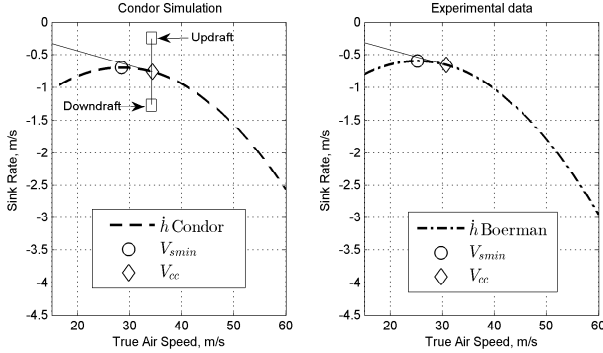

Fig. 5. Identifying the inherent sink polar: both the sink rate and the TAS are directly measured by the onboard sensors. Minimum sink rate $V_s min$ and the optimal crusing speed V_{cc} corresponding to the maximum glide ratio (typical for the "cross-country" flight) are presented.

the sink polar significantly contributes not only to the identification of thermal updrafts, but also to the mission planning of a specific glider, see Piggott [1997] and FAA [2011]. In particular, the polar defines the minimum sink rate $V_s min$ and the corresponding TAS command for the autopilot to follow. While $V_s min$ may be too close to the stall speed V_{stall} and should be avoided ($V_{stall} \approx V_s min$), the effective speed commanded in thermaling mode V_{th} may be slightly higher. The polar also defines the optimal TAS command V_{cc} for the maximum glide ratio flight that is used by the navigation task in planning for the maximum range "cross-country" segment; the tangent line from the origin defines V_{cc}. While the sink polar should be ideally obtained in no-wind environment, its application to the known wind conditions is also straightforward and allows for the calculation of the distances to be traveled in cross-country flight, see more details in Piggott [1997] and FAA [2011].

The total energy approach is also widely used in human piloted soaring flight. It is based on the concept that the mechanical energy E_{tot} of the soaring glider combines the potential energy, $E_p = mgh$, and kinetic energy, $E_k = \frac{m \cdot V^2}{2}$, of the airframe minus the "leakage" of the energy due to the work of the parasitic and induced aerodynamic drag, E_D. For an "aerodynamically clean" glider with an objective to minimize the total energy loss, the control commands of its autopilot will necessarily result in mild variations of the angle of attack, thus leading to the relatively constant parasitic drag and $\dot{E}_D \approx 0$. Consequently, for the total energy and its rate of change over sufficiently long time intervals one can consider the following:

$$E_{tot} = mgh + \frac{m \cdot V^2}{2} - E_D, \quad E = \frac{E_{tot}}{mg},$$

$$\dot{E} = \dot{h} + \frac{V \cdot \dot{V}}{g}, \quad \ddot{E} = \frac{\dot{V}^2 + V \cdot \ddot{V}}{g} + \ddot{h}, \quad (1)$$

where m is the mass of the airframe, g is the gravitational constant, E is the normalized total mechanical energy of the system (also called the specific energy), h is the height, and V is the inertial speed. Therefore, the longitudinal long period oscillations represent the natural tradeoff of kinetic and potential energy while their sum remains nearly constant. As a consequence, in no updraft conditions the rate of change of the total energy $\dot{E} \approx 0$. Therefore, if there is a significant variation of the total energy, then the energy rate will be significantly away from zero thus indicating the energy variation due to updraft or downdraft airflow. In fact, the total energy management just presented is widely used in manned aviation being implemented in the so-called total energy compensating (TEK) variometer, see for example PitLab [2013].

All the components of equation (1) are available in onboard autopilot. Both equations in (1) are included into one Kalman filter along with the inertial and barometric sensors outputs. The resulting energy rate-based solution provides another accurate indication of the updraft event. A comparison of the output of the total energy approach with the output of the TEK variometer $\dot{h}_{TEK}$ is presented next in Figure.6.
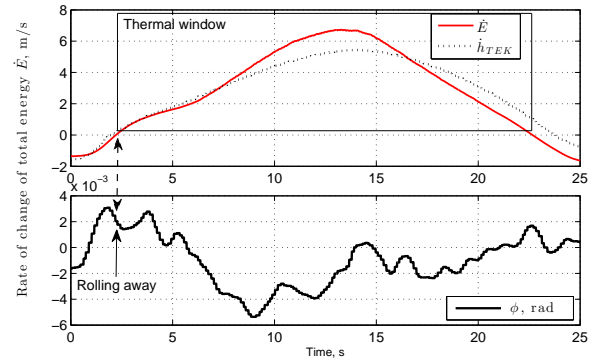

Fig. 6. Energy-based detection of updrafts; the data is simulated by the Condor [2013] software, see sec.4.

2.3 Guidance in Thermal Centering Mode

When a thermal updraft is detected the glider needs to automatically maneuver to enable staying in the thermal with the objective of increasing the glider's potential energy through a rapid increase of the height. The theoretical development of the thermaling guidance law has been recently reported in Andersson et al. [2012b]. The most recent experimental results and findings that motivate further refinement of the solution were discussed in Andersson et al. [2012a]. This development was recently modified to include explicitly the sign of the turn rate command that is defined by the estimate of the body roll angle ϕ; it was observed in a number of flights that entering the thermal induces the motion that rolls the wings away from the thermal, thus suggesting the turn in an opposite direction. The resulting thermaling guidance law implemented onboard of real glider enabled successful latching and effective exploitation of the thermal.

The thermal centering guidance law produces a turn rate command $\dot{\psi}_c$ to the autopilot, and is based on the feedback

control law that takes into account the desire to get closer to the updraft center (defined by the ρ_d), where its intensity (the positive vertical speed) is the highest. On the other hand, the control balances the height increase and the turn-induced sink by a measure proportional to the rate of increase of the total energy (defined by the $\ddot{E}$ in (1)), see the geometry of the guidance task in Figure.7 and the resulting guidance law in (2):

$$\dot{\psi}_c = -sign(\phi) \cdot (\frac{V}{\rho_d} - k_1 \cdot \ddot{E}), \qquad (2)$$

where ρ and ρ_d are the current distance and the desired orbital radius around the center of the thermal updraft, ϕ is the roll angle induced by the updraft, and k_1 is the feedback gain determined by the stability and performance requirements. For the feasibility of theoretical development
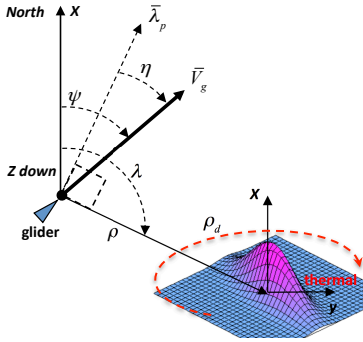

Fig. 7. Kinematics of guidance around a stationary thermal updraft; the desired orbit is represented by the red dashed line defined by ρ_d.

the thermal center is assumed stationary with its position unknown. The desired distance (ρ_d) toward the center at this point is not defined, however for the stability of the control law it is assumed to be away from zero. The best value of ρ_d is initially assigned based on statistical observations of the glider performance and the shapes of updrafts in the area. Later on, when collaborative gliders contribute to the identification of the updraft geometry this value is updated, thus resulting in a feedback that improves the collaborative efficiency of utilizing the free energy of the updraft. For the stability analysis of the thermaling guidance law it is assumed that the intensity of the updraft can be represented by the Gaussian distribution function of the form:

$$\omega = \omega_p \cdot e^{-[\frac{(x-x_0)^2 + (y-y_0)^2}{2\sigma^2}]}, \qquad (3)$$

where x, y represent the coordinates of the glider, x_0, y_o represent the unknown coordinates of the center of updraft, ω_p is the peak intensity of the updraft, and σ defines the geometry of the symmetric updraft (in general case $\sigma_x \neq \sigma_y$). For a stationary updraft modeled by Gaussian distribution function with $\sigma > 0$, $\omega_p > 0$ and the glider with $V > 0, \rho_d > 0$, it is proven that the feedback guidance law in (2) is locally asymptotically stable with an equilibrium at $(\eta, \rho - \rho_d) = (0, 0)$ and a region of attraction $\Omega = \{(\eta, \rho - \rho_d) : |\rho - \rho_d| \leq \beta, |\eta| \leq \alpha\}$, where $\beta < \rho_d, \alpha < \pi/2$, for any

$$k_1 > \tan\alpha \frac{\sigma^2}{\omega_p(\rho_d - \beta)^2} e^{(\frac{-(\rho_d + \beta)^2}{2\sigma^2})}.$$

The physical meaning of the guidance law (2) is to increase the commanded turn rate until the rate of climb in the latched updraft is compensated by the sink resulted from the steep banking; most traditional autopilots implement bank-to-turn control laws.

3. COOPERATIVE ALGORITHMS

The initial approach to the estimation of thermals ($2D$ coordinates of the center vs. the glider altitude) by utilizing the measurements of single glider in soaring mode was based on two classical nonlinear filtering techniques: first - the nonlinear Kalman filter with the "bearings only measurements", and second - the kinematic relation $\dot{\rho} = -V_g \cdot sin(\eta)$ between the speed over ground V_g and the "navigation error" η, see Figure.7. In both formulations the bearing to the updraft center was assumed to be constant at $\pi/2$ ($\lambda - \psi = \pi/2$) with respect to the direction of turning flight; the turn is defined toward the center of the updraft. When entering a strong updraft, the performance of either filter was slow but reasonable, resulting in a converging solution in about 2 full orbits and precision of the thermal center estimation of $75m$.

3.1 Bayesian Mapping of Thermals

To further improve the efficiency of updraft estimation the solution should integrate the knowledge gained by multiple gliders and the prior meteorological observations (see Pennycuick [1998], Hindman et al. [2007]), which might be available for the area of operation. The latter data can be conveniently interpreted as a map of probability density of convective air activity with respect to the geographic latitude and longitude, see a conceptual example in Figure.8. As a first step toward cooperative identifi-
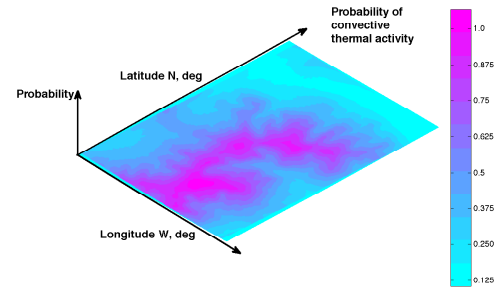

Fig. 8. "Heat map" of probability of finding a thermal over an area of operation.

cation and mapping of convective thermals over extended areas with an account of prior methodological observation, the probabilistic recursive Bayesian approach was adopted, see details of the approach in Bergman [1999].

Consider a task where N gliders cooperatively estimate the velocity $f_k = f(x_k, y_k, z_k)$ of flow field at the inertial coordinates x_k, y_k, z_k of k-th glider, $k = 1...N$. Assume that the onboard instrumentation enables measuring the lateral and vertical components of the airflow. The convective airflow of interest is captured by a given parametric model with unknown characteristics; see, for example, the vertical updraft model in (3) with unknown parameters ω_p, σ, x_0, y_0. The objective of the task is to estimate f by using

noisy observations of the airflow provided by cooperative gliders.

Let $X(t) = (\omega_p, \sigma, x_0, y_0)$ be a state vector that encapsulates the unknown parameters of the convective flow velocity f_k that is estimated at each point of the discretized space at time t, $s_k(t)$ denote the noisy measurement of vehicle k at time t, and $S_k(t) = \{s_k(0), ..., s_k(t)\}$ define the set of samples up to the current time t. Assume that $s_k(t)$ of each vehicle at location x_k, y_k, z_k is corrupted by Gaussian noise such that $s_k(t) = f_k(x_k, y_k, z_k) + \mu_{h,k} + \mu_{v,k}$, with $\mu_{h,k} \sim N(0, \sigma_h^2)$ and $\mu_{v,k} \sim N(0, \sigma_v^2)$ being white noise components in the lateral and vertical directions.

Then, the conditional probability of the state $X(t)$ given the set of measurements $S_k(t)$ of k-th glider is

$$p(X(t)|S_k(t)) = \beta \cdot p(s_k(t)|X) \cdot p(X(t)|S_k(t-1)), \quad (4)$$

where β is the normalization coefficient chosen to guarantee that $p(X(t)|S_k(t))$ at every instance of t has a unity integral over the state-space X. The $p(s_k(t)|X)$ is the likelihood function represented by the conditional probability of the measurement $s_k(t)$ given the state $X = f_k$, and the $p(X(t)|S_k(t-1))$ is the prior probability distribution that represents any given knowledge or intelligence about the most likely location and intensity of thermals. In our development $p(X(t)|S_k(t-1))$ is what encapsulates the probability "heat map", see conceptual Figure.8.

Finally, let each point of state X in the state-space be represented by the multi-variate Gaussian likelihood function:

$$p(s_k(t)|X) = \frac{1}{[2\pi\Delta]^{\frac{1}{2}}} exp(\frac{-[f_k(X) - s_k(t)]}{\sum[f_k(X) - s_k(t)]}),$$

where $\Delta = diag(\mu_h^2, \mu_v^2)$. Assuming that measurements are taken at each time step and the gliders cooperatively share the data, the conditional probability density of the state $X(t)$ is updated through the natural motion of the fleet of gliders sampling the airflow at (x_k, y_k, z_k) as

$$p(X(t)|S(t)) = \beta \cdot \prod_{k=1}^{N} p(s_k(t)|X) \cdot p(X(t)|S(t-1)), \quad (5)$$

where $S(t-1)$ includes the measurements from all N gliders in the fleet. Now it is clear that the points of the parameter space corresponding to the maximum of the posterior probability density $X(t) = \max p(X(t)|S(t))$ provide the maximum likelihood of the convective flow field parameters.

An example of the recursive algorithm (5) for the case of three simulated gliders cooperatively flying and estimating parameters of a single updraft in a given area modelled by (3) is presented in Figure.9. The task is to find the updraft in a bounded area and to converge to the same thermal by utilizing the detection algorithms discussed above; the task mimics the setup and the objectives of our first cooperative flight test of two gliders reported earlier in Andersson et al. [2012b]. In the demonstrated result the prior probability density is initialized by a uniform function over the entire area of operation. The result corresponds to the progression of the probability density function estimated onboard of glider #1 along its
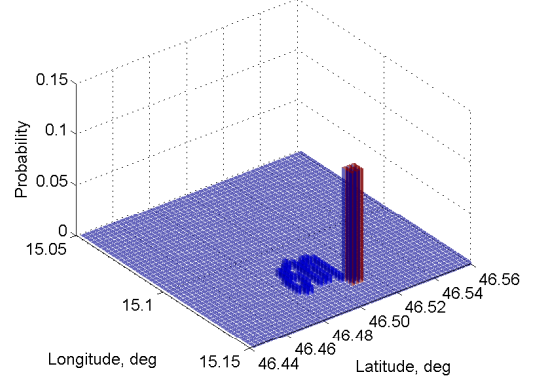

Fig. 9. Estimation of an updraft obtained onboard of glider #1 from the cooperative sampling of environment.
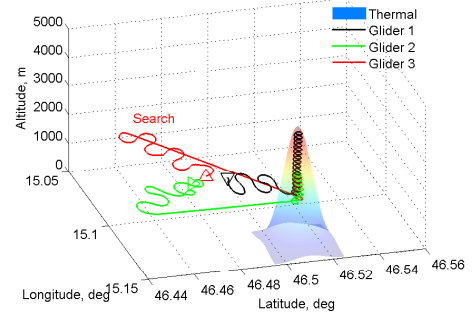

Fig. 10. Cooperative flight of three gliders; starting at different locations they all converge to the same updraft when glider #1 finds it and shares its estimated location.

flight path, see the corresponding cooperative trajectories of gliders #2 and #3 in Figure.10, see more details on the simulation setup in section 4.

4. SIMULATION ENVIRONMENT

To facilitate convenient design and verification of the designed algorithms the project also develops a realistic simulation environment that is based on tight integration of MatLab/Simulink (MATLAB [2013]) capabilities with the high-fidelity flight dynamics and atmospheric effects of the Condor soaring simulator, see Condor [2013]. Besides providing a wide nomenclature of gliders, the software integrates the cooperative behaviors of multiple agents that is essential to the project; the collaboration is enabled by sharing the states of gliders over the network. The architecture of the software in the loop setup is presented in Figure.11.

As an illustration of the achieved capabilities, Figure.10 represents the cooperative flight of three gliders in a simplified scenario introduced above. The gliders start their flight simultaneously at the same altitude, and initially spend some time in search for thermals. When glider #1 detects an updraft utilizing either of the thermal detection approaches (see sec.2.2), and shares the information about the thermal, the other two gliders arrive to the same thermal and successfully gain height all together. Time history of the altitude of three cooperative gliders is presented
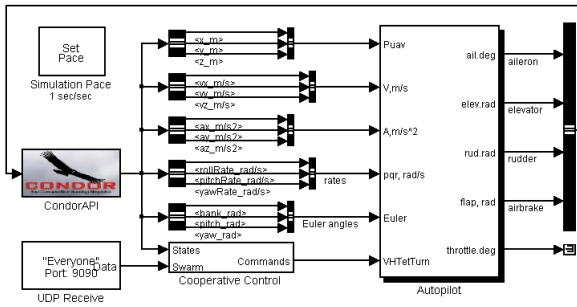
Fig. 11. Integration of Simulink and Condor capabilities.

next in Figure.12. The result clearly demonstrates the benefits and significant potential of collaborative strategies in harvesting the convective updraft energy from the environment.
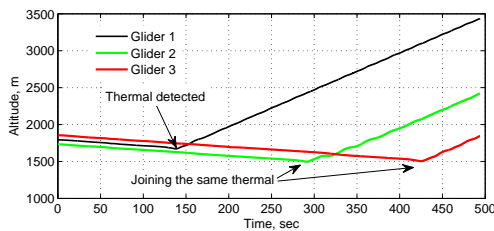

Fig. 12. An example of cooperative flight of three gliders.

5. CONCLUSION

The paper presents the initial development of cooperative convective thermal and solar energy harvesting capability integrated onboard of multiple gliders. The discussion details the key technologies required to integrate the energy harvesting into a cooperative mission planning and execution environment. The key technologies include the online characterization of the electrical (PV solar and batteries) management system, glider properties identification, convective thermals detection, and the collaborative environment sensing by utilizing recursive Bayesian estimation.

REFERENCES

Michael J Allen. Updraft model for development of autonomous soaring uninhabited air vehicles. In *44th AIAA Aerospace Sciences Meeting and Exhibit*, 2006.

Michael J Allen and Victor Lin. Guidance and control of an autonomous soaring vehicle with flight test results. In *AIAA Aerospace Sciences Meeting and Exhibit, AIAA Paper*, volume 867, 2007.

Klas Andersson, Kevin Jones, Vladimir Dobrokhodov, and Isaac Kaminer. Thermal highs and pitfall lows-notes on the journey to the first cooperative autonomous soaring flight. In *Decision and Control (CDC), 2012 IEEE 51st Annual Conference on*, pages 3392–3397. IEEE, 2012a.

Klas Andersson, Isaac Kaminer, Vladimir Dobrokhodov, and Venanzio Cichella. Thermal centering control for autonomous soaring; stability analysis and flight test results. *AIAA Journal of Guidance, Control, and Dynamics*, 35(3):963–975, 2012b.

KJ Astrom and Björn Wittenmark. *Adaptive control*. Addison-Wesley, 1975.

Niclas Bergman. *Recursive Bayesian Estimation*. PhD thesis, Department of Electrical Engineering, Linköping University, Sweden, 1999.

LMM Boermans and A Van Garrel. Design and windtunnel test results of a flapped laminar flow airfoil for high-performance sailplane applications. In *ICAS proceedings*, volume 19, pages 1241–1241. American Institute of Aeronautics and Astronautics, AIAA, 1994.

National Research Council Committee on Autonomous Vehicles in Support of Naval Operations. *Autonomous Vehicles in Support of Naval Operations*. The National Academies Press, 2005. ISBN 9780309096768. URL http://www.nap.edu/.

Condor. The competition soaring simulator, October 2013. URL http://www.condorsoaring.com/.

Daniel J Edwards. Implementation details and flight test results of an autonomous soaring controller. In *AIAA Guidance, Navigation and Control Conference and Exhibit*. North Carolina State University, 2008. AIAA 2008-7244.

Federal Aviation Administration FAA. *Glider Flying Handbook*. JL Aviation LLC, 2011.

Yoshihiro Hamakawa. *Thin-film solar cells: next generation photovoltaics and its applications*, volume 13. Springer, 2004.

Edward Hindman, Stephen M Saleeby, Olivier Liechti, and William R Cotton. A meteorological system for planning and analyzing soaring flights in colorado usa. *Technical Soaring*, 31(3):68–82, 2007.

David R Martinez, Robert A Bond, and M Michael Vai. *High performance embedded computing handbook: A systems perspective*. CRC Press, 2008.

MATLAB. *version 8.2.0.701 (R2013b)*. The MathWorks Inc., Natick, Massachusetts, 2013.

Kenzo Nonami, Muljowidodo Kartidjo, Kwang-Joon Yoon, and Agus Budiyono. *Autonomous Control Systems and Vehicles: Intelligent Unmanned Systems*. Springer Publishing Company, Incorporated, 2013.

CJ Pennycuick. Field observations of thermals and thermal streets, and the theory of cross-country soaring flight. *Journal of Avian Biology*, 29(1):33–43, March 1998.

Derek Piggott. *Gliding: A handbook on soaring flight*. A & C Black, 1997.

PitLab. Skyassistant variometer, October 2013. URL http://www.pitlab.com.

Bruno Siciliano and Oussama Khatib. *Springer handbook of robotics*. Springer, 2008.

Martin Simons and Paul A Schweizer. *Sailplanes by Schweizer: A History*. Crowood Press, 1998.

Gaurav Singh and Sandeep Kumar Shukla. *Low Power Hardware Synthesis from Concurrent Action-Oriented Specifications*. Springer, 2010.

J-M Tarascon and Michel Armand. Issues and challenges facing rechargeable lithium batteries. *Nature*, 414(6861): 359–367, 2001.

Ho-Ming Tong. Microelectronics packaging: present and future. *Materials chemistry and physics*, 40(3):147–161, 1995.

John Wharington. *Autonomous control of soaring aircraft by reinforcement learning*. PhD thesis, Royal Melbourne Institute of Technology (Australia), 1998.